

Establishing an accurate infrared band strength for the cyanate ion in interstellar ices

Perry A. Gerakines, Christopher K. Materese and Reggie L. Hudson*

Astrochemistry Laboratory, NASA Goddard Space Flight Center, Greenbelt, MD 20771, USA

Accepted 2025 January 29. Received 2024 November 22; in original form 2024 October 17

ABSTRACT

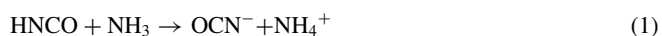
A prominent infrared (IR) spectral feature near 2165 cm^{-1} ($\lambda = 4.62\text{ }\mu\text{m}$) in interstellar ices has been attributed to the cyanate ion (OCN^-) for almost 40 yr, but firm, first-principles solid-phase IR data for quantifying IR-astronomical observations of OCN^- in a H_2O -rich amorphous ice have never been published. Here we report the first laboratory study that delivers such an IR band strength for OCN^- that is reproducible and free of ambiguous uncertainties concerning ice density, thickness, and temperature, providing new quantitative results for both observational and laboratory astronomers. Additional results include the first robust measurements of IR band strengths of isocyanic acid (HNCO), ammonia (NH_3), and the ammonium ion (NH_4^+) in H_2O -rich ice.

Key words: astrochemistry – molecular data – methods: laboratory: molecular – methods: laboratory: solid state – ISM: molecules.

1 INTRODUCTION

Of the features found in the IR spectra of interstellar ices, the most distinct are those from solid H_2O , CO , and CO_2 . Close behind is a band near 2165 cm^{-1} ($\lambda = 4.62\text{ }\mu\text{m}$) that was first reported by Soifer et al. (1979) and first attributed to OCN^- , the cyanate anion, by Grim & Greenberg (1987). Compared to other nitrogen-containing species sometimes assigned to spectral features of interstellar ices, this IR band of the cyanate anion is readily identified and measured due to its distinctive IR position, shape, and width with minimal overlap from other strong absorbances (Boogert et al. 2015). Thus, it is not surprising that in the past 45 yr, OCN^- has been found in ices of a variety of objects including protostars and dense molecular clouds, such as recently by Boogert et al. (2022) and McClure et al. (2023). Cyanate also has been identified in observations towards the Galactic Centre (Chiar et al. 2002) and towards an external galaxy, NGC 4945 (Spoon et al. 2003).

In sharp contrast to the relative ease of observing and identifying interstellar OCN^- with IR methods stands the challenge of measuring abundances of interstellar cyanate, which requires an IR band strength. The only published band strength we have found for OCN^- in amorphous H_2O -ice is that of van Broekhuizen et al. (2004). Those authors warmed HNCO and NH_3 in a H_2O -rich ice to initiate reaction (1) below, and from the amount of NH_3 consumed, determined by IR spectroscopy, the amount of OCN^- produced was found from the reaction’s stoichiometry.



The OCN^- yield, when combined with the accompanying IR spectrum, was used to calculate an IR band strength for OCN^- .

As of this writing (November 2024), the paper of van Broekhuizen et al. (2004) has been cited over a hundred times, but it is not

clear that its limitations have been recognized. For example, the reference band strength for solid NH_3 used to calculate the OCN^- yield was from pioneering work by d’Hendecourt and Allamandola (1986) that lacks details about the number of ices measured, the thicknesses of such ices (if more than one), the refractive index used to measure thicknesses, and how the thickness measurements were made. All ice densities were assumed to be 1 g cm^{-3} , and there is a discrepancy of ~ 57 per cent between the approximation used for areas of the assumed Lorentzian band shapes and the actual equation for Lorentzian band areas (Hudson et al. 2024a).

The paper of van Broekhuizen et al. (2004) also has problems in not stating the number of ices examined, their sizes (i.e. thickness), integration ranges of IR bands, and how changes in IR band areas due to reaction (1) were deconvoluted from changes due simply to the authors’ variations of temperature (15 to 122 K). Moreover, there was an assumption that the reference band strength for anhydrous solid NH_3 was unchanged when H_2O -ice was present, and the method for making multicomponent ices and ensuring the accuracy of their composition was not explained. To these concerns we can add that the use of a large NH_3 excess in the ices of van Broekhuizen et al. (2004) is unfortunate as it led to results based on small differences in large numbers (NH_3 column densities). Ammonia itself is a poor choice as a reference because the IR band followed, near 1100 cm^{-1} , sits near the large libration band of H_2O -ice. Finally, the results of van Broekhuizen et al. (2004) were based on warming an ice and following the decrease of the NH_3 absorbance near 1100 cm^{-1} , but fig. 1 of that paper shows IR spectra at 15, 52, and 122 K with no apparent decrease in intensity of that NH_3 band.

Faced with these problems, here we report measurements of the IR band strength of the OCN^- feature at 2165 cm^{-1} ($\lambda = 4.62\text{ }\mu\text{m}$) in an amorphous H_2O -rich ice. Our work is based on reaction (1), but with HNCO as the reference material, supported by the first accurate measurements of its band strength that are based on the first determinations of the density and refractive index of amorphous HNCO . In addition, we also report new measurements of

* E-mail: reggie.hudson@nasa.gov

IR intensities of HNCO , NH_3 , and NH_4^+ in amorphous H_2O -rich ice. Our results will allow the quantification of these nitrogen-containing species in interstellar ices and laboratory analogues with an accuracy heretofore impossible.

2 LABORATORY METHODS

The methods, procedures, and equipment used have been described in publications from our group over the past 15 yr, most recently in papers such as Hudson et al. (2017), Yarnall & Hudson (2022), Gerakines et al. (2023), and Hudson et al. (2024a). Conventional vacuum line and gas-phase deposition methods (CsI substrate, background pressure $\sim 10^{-8}$ to 10^{-9} Torr) were used to make ices, with transmission IR spectra being recorded with a resolution of 1 cm^{-1} (200 scans). A few measurements were made at a resolution of 0.5 cm^{-1} , but no significant differences were found from our choice of 1 cm^{-1} . In short, our results were not resolution limited. Interference fringes recorded during ice growth permitted ice thicknesses to be determined. Growth rates (ice thickness increase) were on the order of $1 \mu\text{m h}^{-1}$.

Refractive indices and densities of ices, for determining thicknesses and IR intensities, were measured in a UHV chamber ($\sim 10^{-10}$ Torr) with two-laser interferometry (Tempelmeier & Mills 1968) and a quartz-crystal microbalance (Lu & Lewis 1972), respectively. Triplicate measurements gave $n(670 \text{ nm}) = 1.344 \pm 0.005$ and $\rho = 1.102 \text{ g} \pm 0.005 \text{ g cm}^{-3}$ for solid HNCO at 19 K. Similar data for NH_3 and other amorphous solids can be found in Hudson et al. (2020).

Isocyanic acid was synthesized by condensing HCl gas (Matheson) onto dry sodium cyanate, NaOCN (Sigma Aldrich) in a vacuum line (e.g. Cottin et al. 2003). An ethanol cryogenic bath at 155 K was used to remove residual CO_2 , although a trace of CO_2 remained at a concentration below 0.4 percent in a few ices. Experiments with H_2O -ice used triply distilled H_2O with a resistivity greater than 10^7 ohm-cm and which was degassed with freeze-pump-thaw cycles using liquid nitrogen. Research-grade ammonia (NH_3) was obtained from Matheson and used as received.

Band strength (A') uncertainties are ~ 5 percent (Gerakines et al. 2023; Hudson et al. 2024a). See also Hudson & Yarnall (2022) for methods used for this estimate.

Radiation experiments were conducted with H_2O -rich ices formed on a ZnSe substrate, and used the same Van de Graaff accelerator employed in our earlier work (e.g. Moore & Hudson 1998; Hudson & Ferrante 2019), delivering 0.9 MeV protons with a beam current of $\sim 1 \times 10^{-7} \text{ A}$. Radiation doses were measured by a calibrated metal ring on the sample holder and were 1–25 MGy using a stopping power of $255 \text{ MeV cm}^2 \text{ g}^{-1}$ calculated with Ziegler's SRIM software, a density of 1 g cm^{-3} , and no compound correction (Ziegler 2013).

3 RESULTS

3.1 IR band strengths

The upper and middle panels of Fig. 1 show IR transmission spectra of two amorphous ices at 10 K, neat HNCO and $\text{H}_2\text{O} + \text{HNCO}$ (10:1). Here we are concerned only with the strong IR absorbance near 2250 cm^{-1} , the asymmetric NCO stretching mode of HNCO . In a separate publication, we consider the entire mid-IR spectrum of both amorphous and crystalline HNCO including band strengths and optical constants (Hudson et al. 2024b).

Infrared spectra of six amorphous HNCO ices with thicknesses from about 0.12 to $1.25 \mu\text{m}$ were recorded and used to construct a Beer's Law plot for HNCO at 10 K, from which a band strength A' was calculated by the standard method introduced by Hollenberg &

Dows (1961). See also many of our recent publications, such as Gerakines et al. (2024). The result for HNCO was $A' (2250 \text{ cm}^{-1}, 10 \text{ K}) = 1.29 \times 10^{-16} \text{ cm molecule}^{-1}$.

The $\text{H}_2\text{O} + \text{HNCO}$ (10:1) ice of Fig. 1 (middle panel) was prepared and quantified using the method of Yarnall & Hudson (2022). Specifically, separate pre-calibrated deposition lines were used to prepare seven $\text{H}_2\text{O} + \text{HNCO}$ (10:1) ices with thicknesses from about 0.1 to $1 \mu\text{m}$. The resulting Beer's Law plot for the absorbance near 2250 cm^{-1} is shown in the bottom panel of Fig. 1. The line's slope is the HNCO band strength, $A' (2257 \text{ cm}^{-1}, 10 \text{ K}) = 9.79 \times 10^{-17} \text{ cm molecule}^{-1}$.

The top panel of Fig. 2 shows a spectrum of a three-component ice, $\text{H}_2\text{O} + \text{HNCO} + \text{NH}_3$, with a composition of about 10:1:1. To make this sample, HNCO was condensed onto a 10-K CsI substrate simultaneously with $\text{H}_2\text{O} + \text{NH}_3$ ($\sim 10:1$) from a separate deposition line, the deposition rate for each line having been adjusted beforehand to give the desired composition. The resulting IR spectrum resembles that of $\text{H}_2\text{O} + \text{HNCO}$ in Fig. 1, but the OCN^- feature near 2165 cm^{-1} is now present as are absorptions from NH_3 and NH_4^+ . The middle panel of the same figure shows spectra as the ice was held at 10 K for several hours in the IR beam, the HNCO feature decreasing, and the OCN^- band increasing. In other words, reaction (1) took place.

The bottom panel of Fig. 2 shows that during the $\text{HNCO} \rightarrow \text{OCN}^-$ reaction the changes in areas of the two bands were proportional by a constant factor as the HNCO feature fell and the OCN^- band rose. Knowing the band strength of HNCO in H_2O -ice (*vide supra*) the band strength of OCN^- was calculated to be $A' (2170 \text{ cm}^{-1}, 10 \text{ K}) = 1.51 \times 10^{-16} \text{ cm molecule}^{-1}$. The measurements for the bottom panel of Fig. 2 were made at roughly 1-h intervals over 20 h. For information on the reaction's rate, see Mispelaer et al. (2012) and references therein.

Table 1 summarizes the band strengths measured for HNCO and OCN^- at 10 K, each being the first accurate, reproducible measurement of its type.

Our primary goal in this study was determining an accurate band strength for OCN^- using HNCO 's band strength, but it seemed reasonable to also consider the other molecule and ion in equation (1), NH_3 and NH_4^+ . We already have published $A'(\text{NH}_3, 1071 \text{ cm}^{-1}, 10 \text{ K}) = 1.95 \times 10^{-17} \text{ cm molecule}^{-1}$ for amorphous NH_3 near 10 K (Hudson et al. 2022). Following the procedure used for $\text{H}_2\text{O} + \text{HNCO}$ in Fig. 1, we prepared four ices (thickness from about 0.25 to $1 \mu\text{m}$) of $\text{H}_2\text{O} + \text{NH}_3$ (10:1) and recorded their IR spectra, focusing on the so-called umbrella mode of NH_3 near 1100 cm^{-1} . The usual analysis gave $A'(1117 \text{ cm}^{-1}, 10 \text{ K}) = 1.47 \times 10^{-17} \text{ cm molecule}^{-1}$ for NH_3 in the $\text{H}_2\text{O} + \text{NH}_3$ (10:1) ices. For NH_4^+ , the spectra in Fig. 2 also showed an increase in the area of the NH_4^+ feature near 1481 cm^{-1} over time. A comparison of that increase to the decrease in area for the HNCO band gave $A'(1481 \text{ cm}^{-1}, 10 \text{ K}) = 5.94 \times 10^{-17} \text{ cm molecule}^{-1}$ for NH_4^+ in the three-component ice, $\text{H}_2\text{O} + \text{HNCO} + \text{NH}_3$ ($\sim 10:1:1$). Again, Table 1 summarizes the results.

3.2 An application – radiolysis of HNCO

Laboratory studies have shown that OCN^- can form in ices in several ways. Examples include acid-base reactions (Raunier et al. 2003), ice photolysis (Lacy et al. 1984; Demyk et al. 1998), and radiation-chemical studies (Hudson et al. 2001; Bennett et al. 2010). A useful, but dated, compilation of such work is given by van Broekhuizen et al. (2005). The IR studies of cyanate formation listed there, and all subsequent studies, have one thing in common: they all lack a

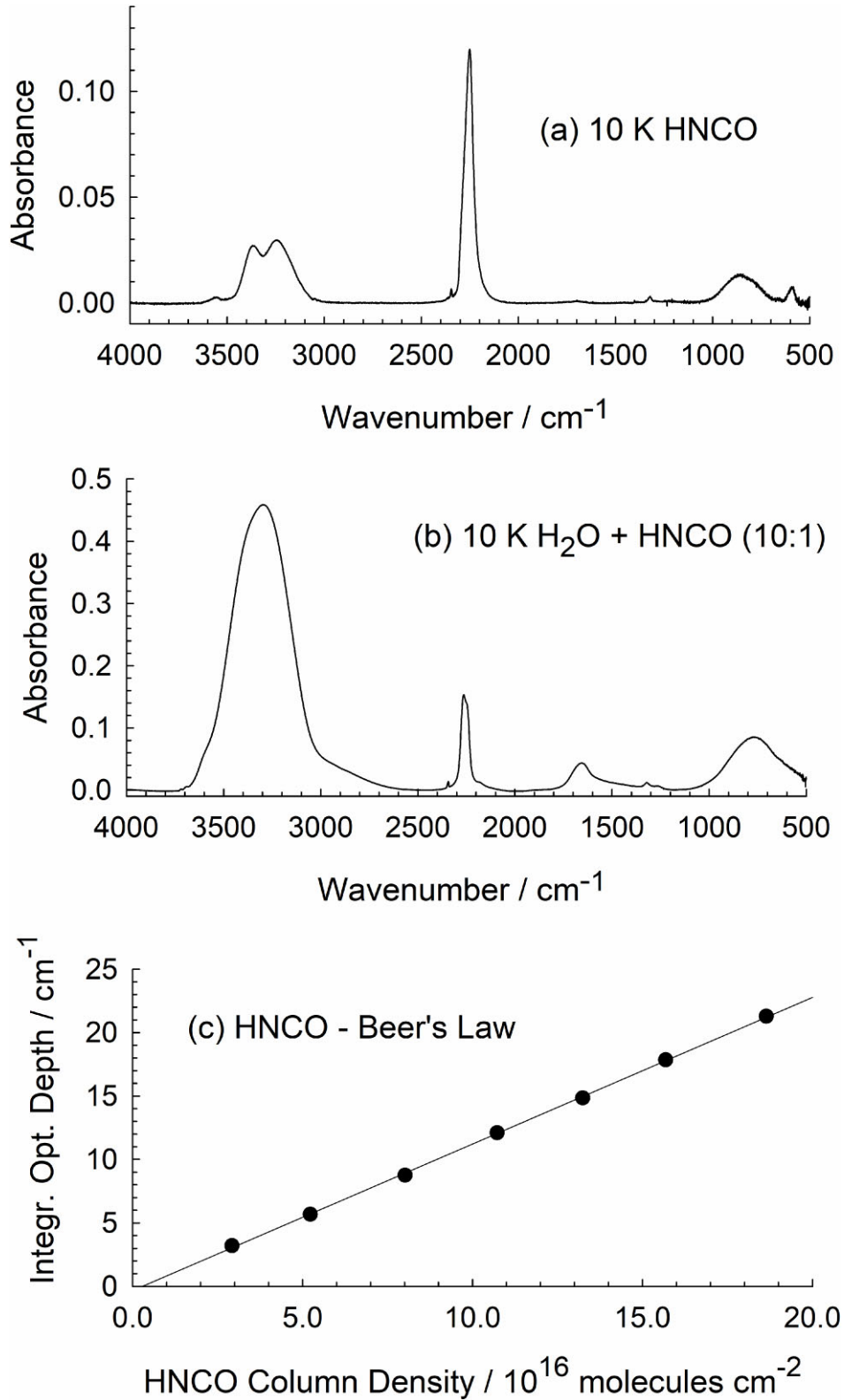


Figure 1. (a) IR spectrum of amorphous HNC0 at 10 K, (b) IR spectrum of amorphous H₂O + HNC0 (10:1) at 10 K, and (c) Beer's Law plot for the NCO asymmetric stretching mode of HNC0 in H₂O + HNC0 (10:1) at 10 K. The ice thicknesses in (a) and (b) were about 0.1 and 0.8 μm , respectively.

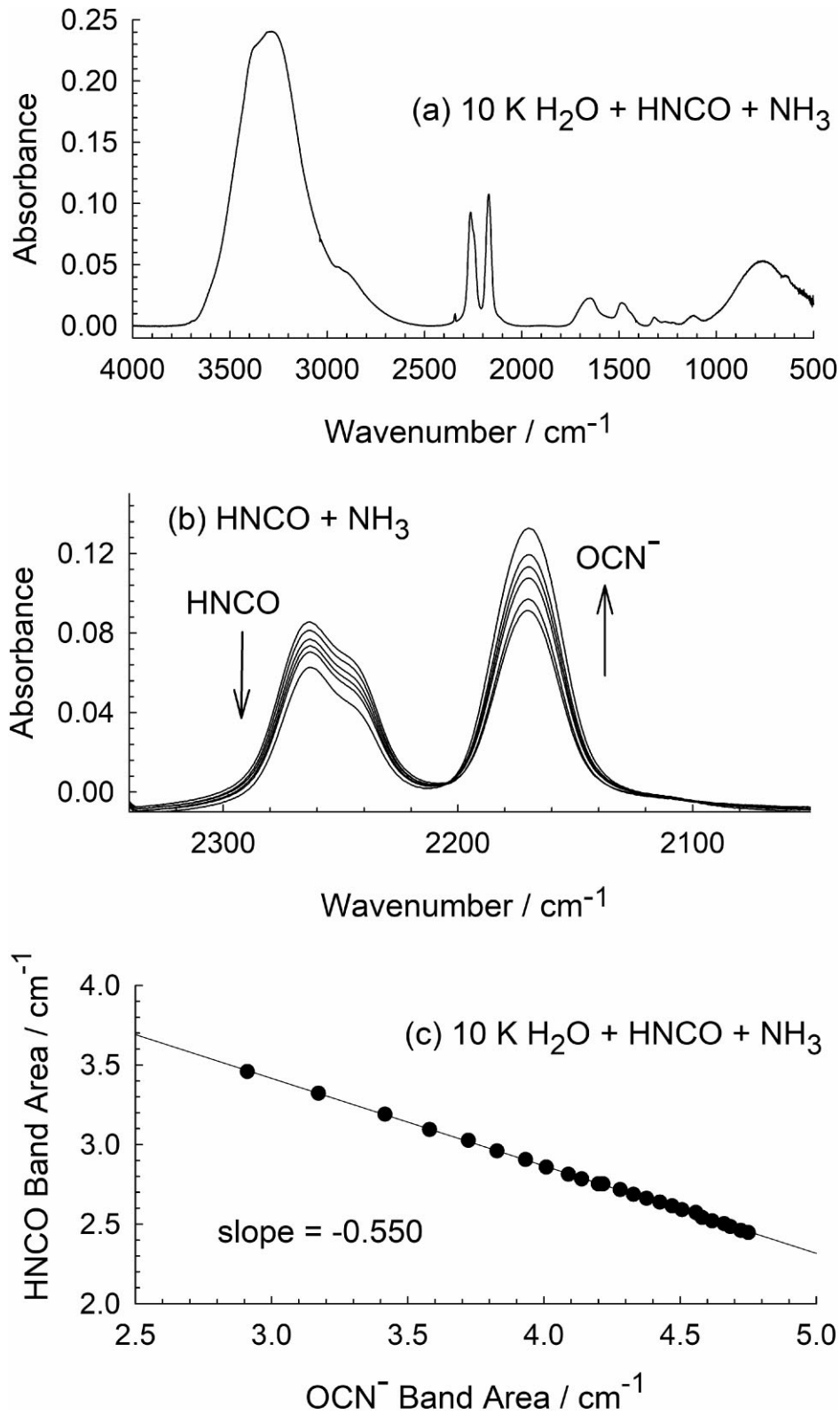


Figure 2. (a) IR spectrum of $\text{H}_2\text{O} + \text{HNCO} + \text{NH}_3$ (~10:1:1) at 10 K, (b) expansion of the same showing changes in band areas on sitting at 10 K, and (c) band areas of HNCO and OCN^- on sitting at 10 K in the IR beam. The ice's original thickness was about 1 μm .

Table 1. Intensities of mid-IR absorptions of amorphous ices at 10 K^a

Species	Ice	Position $\bar{\nu}/\text{cm}^{-1}$	Position $\lambda/\mu\text{m}$	Integration range/ cm^{-1}	$A'/10^{-18}$ cm molecule ⁻¹
HNCO	Neat HNCO	2250	4.444	2400–2100	129
HNCO	H ₂ O + HNCO (10:1)	2255 ^b	4.435	2363–2211 ^c	97.9
OCN ⁻	H ₂ O + HNCO + NH ₃ (~10:1:1)	2170	4.608	2211–2100	151
NH ₃	Neat NH ₃	1071	9.337	1300–950	19.5 ^d
NH ₃	H ₂ O + NH ₃ (10:1)	1117	8.953	1220–1050	14.7
NH ₄ ⁺	H ₂ O + HNCO + NH ₃ (~10:1:1)	1481	6.752	1538–1388	59.4

^aValues of A' are rounded to three significant figures. See Section 2 of the text for uncertainties.

^bPosition of centre of band.

^cSmall area of CO₂ band subtracted.

^dSee Hudson et al. (2022).

firmly established IR band strength with which to quantify OCN⁻ yields.

To demonstrate the use of our new results, we irradiated an H₂O + HNCO (10:1) ice at 20 K and quantified the subsequent HNCO-to-OCN⁻ conversion by IR spectroscopy. The upper panel of Fig. 3 shows spectra in the relevant region before and after irradiation of the sample with 0.9 MeV p⁺ to a dose of 25 MGy. A decrease in the HNCO band and an increase in the OCN⁻ feature are seen with increasing dose. The figure's lower panel shows the changes in column density for HNCO and OCN⁻ in the ice with increasing dose, the column densities being calculated with the band strengths reported here. The rise in OCN⁻ accounts for about 20 per cent of the loss of HNCO loss. The dose rate for a dense molecular cloud is on the order of 120 Gy per year (Moore et al. 2001), so the final dose of 25 MGy in Fig. 3 corresponds to an exposure time of ~200 000 yr.

4 DISCUSSION

The cyanate anion is one of the few nitrogen-containing components that have been assigned to spectral features of interstellar ices in the nearly 50 yr since such spectra were first published (Merrill et al. 1976). Our earlier laboratory work showed how OCN⁻ can be produced by the radiolytic decomposition of larger molecules, by dissociative electron capture by a cyanate, and by either the radiolysis or photolysis of multicomponent ices made of CO and nitrogen-containing molecules (Hudson et al. 2001). Similar results have been reported by others both before (Lacy et al. 1984; Demyk et al. 1998) and after (Bennett et al. 2010) us. However, despite many laboratory observations of OCN⁻, accurate quantification has been impossible due to the lack of supporting laboratory measurements. Here we have reported the first IR band strength of OCN⁻ at 10 K, as well as new measurements of IR intensities of HNCO, NH₃, and NH₄⁺, all in H₂O-rich ice, removing a significant obstacle to quantifying all four species. Our work has been greatly aided by using HNCO as the reference material for reaction (1), which removes the disadvantages and problems of earlier work that adopted NH₃ as the reference.

As stated earlier, the only published band strength we have found for OCN⁻ is from van Broekhuizen et al. (2004) with the problems described in our Introduction. The authors of that paper claimed an accuracy of 20 per cent for their A' value, but no reference or other basis for that accuracy was given. We find that the difference in $A'(\text{OCN}^-)$ between the published value (van Broekhuizen et al. 2004) and that in Table 1 is about 16 per cent. However, that literature value of $A'(\text{OCN}^-)$ is based on a reference band strength for NH₃ of $A'(1070 \text{ cm}^{-1}) = 1.7 \times 10^{-17} \text{ cm molecule}^{-1}$ that itself is suspect. It seems to have gone unreported in the nearly 40

yr since that NH₃ band strength was published (d'Hendecourt & Allamandola 1986) that those authors' equation for the area of the assumed Lorentzian band shape is missing a coefficient of $\pi/2 \approx 1.57$ (Seshadri & Jones 1963; Petrakis 1967). Also, the density of amorphous NH₃ was assumed to be 1.00 g cm⁻³, but a measured density of 0.76 g cm⁻³ at 20 K was available at the time (Wood & Roux 1982). Multiplying the reference A' for NH₃ in d'Hendecourt & Allamandola (1986) by 1.57 and dividing it by 0.76 raises it to $A'(\text{NH}_3, 1070 \text{ cm}^{-1}) = 3.5 \times 10^{-17} \text{ cm molecule}^{-1}$. This allows the $A'(\text{OCN}^-)$ of van Broekhuizen et al. (2004) to be rescaled as $(3.5 \times 10^{-17} \text{ cm molecule}^{-1}) \times (1.3 \times 10^{-16} \text{ cm molecule}^{-1}) / (1.7 \times 10^{-17} \text{ cm molecule}^{-1}) = 2.7 \times 10^{-16} \text{ cm molecule}^{-1}$, which is about 80 per cent above our value in Table 1.

The two comparisons just described are based on the use of anhydrous NH₃ as a reference for measurements of H₂O-rich amorphous ices by van Broekhuizen et al. (2004). Yet another comparison comes from using our band strength for NH₃ in H₂O-rich amorphous ice (Table 1) as a reference. In that case, the per cent differences between the published $A'(\text{OCN}^-)$ and our result is about 34 per cent.

We note in passing one other concern. The reference NH₃ band strength $A'(1070 \text{ cm}^{-1}) = 1.7 \times 10^{-17} \text{ cm molecule}^{-1}$ of d'Hendecourt & Allamandola (1986) has been used by many authors over the past 38 yr, such as from Sandford & Allamandola (1993) to van Broekhuizen et al. (2004) to recently by Canta et al. (2023). However, that same band strength disagrees with what one calculates using the results and method of d'Hendecourt & Allamandola (1986), namely $A'(1070 \text{ cm}^{-1}) = 1.35 \times 10^{-17} \text{ cm molecule}^{-1}$. It is not known if the discrepancy is from a typographical error or a mistake in arithmetic.

Given the many problems, ambiguities, and uncertainties associated with the earlier measurements, we suggest that little should be made of either how close to or far from the resulting A' values are to our results in Table 1. The many unknowns in the earlier work hinder meaningful quantitative comparisons to the extent that any agreements or disagreements can be considered coincidental, but little more.

We have not found any published IR intensity measurements for H₂O + HNCO ices for comparison to our $1.16 \times 10^{-16} \text{ cm molecule}^{-1}$. The spectrum of an H₂O + HNCO ice at 25 K published by Lowenthal et al. (2002) resembles that in the middle panel of our Fig. 1, but neither an ice thickness nor band strengths were provided. In the same paper, Lowenthal et al. (2002) reported a band strength for crystalline HNCO at 145 K, in the absence of H₂O-ice, for the same feature that we measured for an amorphous ice at 10 K (Table 1). The differences in structure and temperatures of the two ices preclude a meaningful comparisons of band strengths. Unfortunately, the paper of Lowenthal et al. (2002) has significant problems starting with the

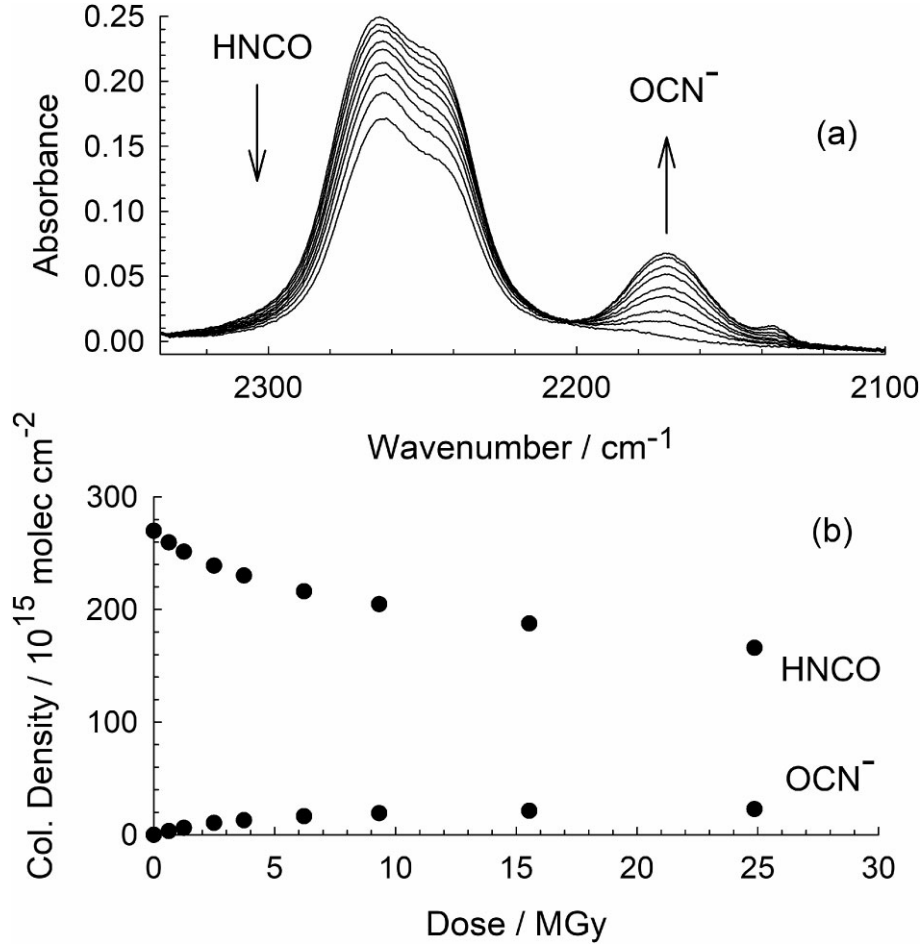


Figure 3. (a) IR spectra of $\text{H}_2\text{O} + \text{HNCO}$ ($\sim 10:1$) at 20 K before and after 0.9 MeV irradiations for doses up to 25 MGy, (b) changes in column densities of HNCO and OCN^- with increasing radiation dose. The ice’s original thickness was about 1 μm . Note that the area of the small CO feature near 2135 cm^{-1} was subtracted from the larger OCN^- band before calculating the latter’s column density.

fact that the IR spectrum shown for HNCO at 20 K is significantly different both from ours in Fig. 1 and the one published by Raunier et al. (2003), no integration limits were given, and there was no indication that more than one ice and thickness were examined by the authors. These concerns with HNCO will be addressed in a separate publication (Hudson et al. 2024b). We also note that the spectra in figs 1 and 3 of Lowenthal et al. (2002) need to be swapped to match the figure captions.

Comments already made for OCN^- also apply to NH_4^+ . The earlier work of van Broekhuizen et al. (2004) on warming an ice gave a band strength that must be raised about 45 per cent to match that reported here for 10 K. However, the ambiguities and omissions of that paper make it difficult to judge the significance of that difference.

In short, we do not recommend the older work of either Lowenthal et al. (2002) or van Broekhuizen et al. (2004) for quantifying IR observations of interstellar ices due to the many difficulties and concerns associated with the procedures, data, and analyses in those papers. The new results presented here will allow firmer, more reliable quantifications by infrared astronomers.

Concerning our radiation-chemical experiment, each 0.9 MeV p^+ passing through our $\text{H}_2\text{O} + \text{HNCO}$ (10:1) ice generated thousands of secondary electrons. Their scavenging by HNCO will play a large part in that molecule’s destruction and the accompanying formation of cyanate by dissociative electron capture, cyanate being a stable

closed-shell leaving group. See reaction (2).



About 20 per cent of the HNCO lost by the irradiation was accounted for by cyanate formation, leaving the balance for other reaction products. Among the products that might be expected from HNCO are formamide ($\text{H}_2\text{NC(O)H}$) by reduction, CO by dissociation, carbamic acid (H_2NCOOH) by hydration, NH_3 from carbamic acid dissociation, and CO_2 formation from both CO and carbamic acid. These products were not studied in this work, our focus being on band strengths and the HNCO -to- OCN^- conversion.

For laboratory astrochemists, our results will allow similar quantification of changes in HNCO and OCN^- either as reactants or products. Our own experience is that OCN^- is produced and can be identified in almost any radiolysis or photolysis experiment involving CO and nitrogen- and hydrogen-containing species as either reactants or products (e.g. Hudson et al. 2001; Hudson & Moore 2004). This is not surprising given the stability of this inorganic anion and the strength of its asymmetric stretching vibration, even greater in intensity than that of CO_2 (Gerakines and Hudson 2015), an isoelectronic counterpart. As for the conjugate acid, HNCO , our work suggests that the lack of an HNCO identification in interstellar ices is not due to a small band strength, but rather to a low HNCO column density.

We end with some suggestions for future work. We have presented results from one type of radiation-chemical experiment. It would be interesting to quantify $\text{HNCO} \rightarrow \text{OCN}^-$ reaction yields from radiolysis and photolysis and to compare them with, for example, the radiolytic or photochemical reduction of isocyanic acid to make formamide, $\text{HNCO} \rightarrow \text{HC(=O)NH}_2$. The quantification of the solid-phase oxidation $\text{OCN}^- \rightarrow \text{CO}_2$ by either radiolysis or photolysis is also of interest. Finally, we mention the paper of Mispelaer et al. (2012). Those authors invoked quantum-mechanical tunnelling to help explain the temperature-independent rate observed below 15 K for the $\text{HNCO} \rightarrow \text{OCN}^-$ reaction. One sign of tunnelling is indeed a curved Arrhenius plot (Bell 1935; Hudson et al. 1977), but H^+ tunnelling should also be accompanied by a large deuterium isotope effect (e.g. Sprague 1977; Williams & Sprague 1982; Macoas et al. 2003). We are unaware of relevant work on the rate of the $\text{DNCO} + \text{ND}_3 \rightarrow \text{OCN}^- + \text{ND}_4^+$ reaction.

5 SUMMARY AND CONCLUSIONS

More than 40 yr after the first observation of interstellar OCN^- , an accurate IR band strength has now been measured for OCN^- in H_2O -rich ice using established laboratory procedures and with explicit attention to the required physical properties of refractive index, density, temperature, and ice composition. The results presented here should be used to quantify cyanate observations with the *JWST* and other infrared observatories.

ACKNOWLEDGEMENTS

We acknowledge the support of NASA's Planetary Science Division Internal Scientist Funding Program through the Fundamental Laboratory Research (FLaRe) work package at the NASA Goddard Space Flight Center with additional funding from the NASA Astrobiology Institute's Goddard Center for Astrobiology. Yukiko Y. Yarnall assisted with a few measurements.

DATA AVAILABILITY

Data underlying this article will be shared on reasonable request to the corresponding author. On acceptance of this manuscript for publication, HNCO spectra will be posted at <https://science.gsfc.nasa.gov/691/cosmicice/spectra.html> on the authors' website.

REFERENCES

- Bell R. P., 1935, *Proc. R. Soc. London A*, 148, 241
 Bennett C. J., Jones B., Knox E., Perry J., Kim Y. S., Kaiser R. I., 2010, *ApJ*, 723, 641
 Boogert A. C. A., Brewer K., Brittain A., Emerson K. S., 2022, *ApJ*, 941, 1
 Boogert A. C. A., Gerakines P. A., Whittet D. C. B., 2015, *Ann. Rev. Astron. Astrophys.*, 53, 541
 Canta A., Oberg K., Mahesh R., 2023, *ApJ*, 953, 1
 Chiar J. E. et al., 2002, *ApJ*, 570, 198

- Cottin H., Moore M. H., Benilan Y., 2003, *ApJ*, 590, 874
 d'Hendecourt L. B., Allamandola L. J., 1986, *A&ASS*, 64, 453
 Demyk K., Dartois E., d'Hendecourt L., Jourdain de Muizon M., Heras A. M., Breitfellner M., 1998, *A&A*, 339, 553
 Gerakines P. A., Hudson R. L., 2015, *ApJ*, 808, L40
 Gerakines P. A., Materese C. K., Hudson R. L., 2023, *MNRAS*, 526, 4051
 Gerakines P. A., Yarnall Y. Y., Hudson R. L., 2024, *Icarus*, 413, 116007
 Grim R. J. A., Greenberg J. M., 1987, *ApJ*, 321, L91
 Hollenberg J. L., Dows D. A., 1961, *J. Chem. Phys.*, 34, 1061
 Hudson R. L., Ferrante R. F., 2019, *MNRAS*, 492, 283
 Hudson R. L., Gerakines P. A., Yarnall Y. Y., 2022, *ApJ*, 925, 1
 Hudson R. L., Gerakines P. A., Yarnall Y. Y., 2024a, *ApJ*, 970, 1
 Hudson R. L., Loeffler M. J., Ferrante R. F., Gerakines P. A., Coleman F. M., 2020, *ApJ*, 891, 22
 Hudson R. L., Loeffler M. J., Gerakines P. A., 2017, *J. Chem. Phys.*, 146, 0243304
 Hudson R. L., Moore M. H., 2004, *Icarus*, 172, 466
 Hudson R. L., Moore M. H., Gerakines P. A., 2001, *ApJ*, 550, 1140
 Hudson R. L., Shiotani M., Williams F., 1977, *Chem. Phys. Lett.*, 48, 193
 Hudson R. L., Yarnall Y. Y., 2022, *ACS E&S Sci.*, 6, 1163
 Hudson R. L., Yarnall Y. Y., Gerakines P. A., 2024b, *ApJ*, 970, 108
 Lacy J. H. et al., 1984, *ApJ*, 276, 533
 Lowenthal M. S., Khanna R. K., Moore M. H., 2002, *Spectrochim. Acta A*, 58, 73
 Lu C. S., Lewis O., 1972, *J. Appl. Phys.*, 43, 4385
 Macoas E. M. S., Khriachtchev L., Pettersson M., Fausto R., Räsänen M., 2003, *J. Amer. Chem. Soc.*, 125, 16188
 McClure M. K. et al., 2023, *Nat. Astron.*, 7, 431
 Merrill K. M., Russell R. W., Soifer B. T., 1976, *ApJ*, 207, 763
 Mispelaer F., Theule P., Duvernay F., Roubin P., Chiavassa T., 2012, *A&A*, 540, A40
 Moore M. H., Hudson R. L., 1998, *Icarus*, 135, 518
 Moore M. H., Hudson R. L., Gerakines P. A., 2001, *Spectrochim. Acta A*, 57, 843
 Petrakis L., 1967, *J. Chem. Educ.*, 44, 432
 Raunier S., Chiavassa T., Marinelli F., Allouche A., Aycard J. P., 2003, *Chem. Phys. Lett.*, 368, 594
 Sandford S. A., Allamandola L. J., 1993, *ApJ*, 417, 815
 Seshadri K. S., Jones R. N., 1963, *Spectrochim. Acta*, 19, 1013
 Soifer B. T., Puetter R. C., Russel R. W., Willner S. P., Harvey P. M., Gillet F. C., 1979, *ApJ*, 232, L53
 Spoon H. W. W. et al., 2003, *A&A*, 402, 499
 Sprague E. D., 1977, *J. Phys. Chem.*, 81, 516
 Tempelmeyer K. E., Mills D. W., 1968, *J. Appl. Phys.*, 39, 2968
 van Broekhuizen F. A., Keane J. V., Schutte W. A., 2004, *A&A*, 415, 425
 van Broekhuizen F. A., Pontoppidan K. M., Fraser H. J., van Dishoeck E. F., 2005, *A&A*, 441, 249
 Williams F., Sprague E. D., 1982, *Acc. Chem. Res.*, 15, 408
 Wood B. E., Roux J. A., 1982, *J. Opt. Soc. Amer.*, 72, 720
 Yarnall Y. Y., Hudson R. L., 2022, *ApJ*, 91, L4
 Ziegler J. F., 2013, *Stopping and Range of Ions in Matter SRIM 2008*, Available at: <http://www.srim.org>

This paper has been typeset from a Microsoft Word file prepared by the author.